AMH/MIS as a contraceptive that protects the ovarian reserve during chemotherapy

Motohiro Kano[a,b], Amanda E. Sosulski[a,b], LiHua Zhang[a,b], Hatice D. Saatcioglu[a,b], Dan Wang[c], Nicholas Nagykery[a,b], Mary E. Sabatini[d], Guangping Gao[c], Patricia K. Donahoe[a,b,1], and David Pépin[a,b,1]

[a]Pediatric Surgical Research Laboratories, Massachusetts General Hospital, Boston, MA 02114; [b]Department of Surgery, Harvard Medical School, Boston, MA 02115; [c]Horae Gene Therapy Center, University of Massachusetts Medical School, Worcester, MA 01655; and [d]Department of Obstetrics and Gynecology, Harvard Medical School and Massachusetts General Hospital, Boston, MA 02114

Contributed by Patricia K. Donahoe, December 29, 2016 (sent for review December 16, 2016; reviewed by Richard N. Freiman, Bruce D. Murphy, and Teresa K. Woodruff)

The ovarian reserve represents the stock of quiescent primordial follicles in the ovary which is gradually depleted during a woman's reproductive lifespan, resulting in menopause. Müllerian inhibiting substance (MIS) (or anti-Müllerian hormone/AMH), which is produced by granulosa cells of growing follicles, has been proposed as a negative regulator of primordial follicle activation. Here we show that long-term parenteral administration of superphysiological doses of MIS, using either an adeno-associated virus serotype 9 (AAV9) gene therapy vector or recombinant protein, resulted in a complete arrest of folliculogenesis in mice. The ovaries of MIS-treated mice were smaller than those in controls and did not contain growing follicles but retained a normal ovarian reserve. When mice treated with AAV9/MIS were paired with male breeders, they exhibited complete and permanent contraception for their entire reproductive lifespan, disrupted vaginal cycling, and hypergonadotropic hypogonadism. However, when ovaries from AAV9-MIS–treated mice were transplanted orthotopically into normal recipient mice, or when treatment with the protein was discontinued, folliculogenesis resumed, suggesting reversibility. One of the important causes of primary ovarian insufficiency is chemotherapy-induced primordial follicle depletion, which has been proposed to be mediated in part by increased activation. To test the hypothesis that MIS could prevent chemotherapy-induced overactivation, mice were given carboplatin, doxorubicin, or cyclophosphamide and were cotreated with AAV9-MIS, recombinant MIS protein, or vehicle controls. We found significantly more primordial follicles in MIS-treated animals than in controls. Thus treatment with MIS may provide a method of contraception with the unique characteristic of blocking primordial follicle activation that could be exploited to prevent the primary ovarian insufficiency often associated with chemotherapy.

MIS | AMH | oncofertility | AAV9 | contraceptive

Müllerian inhibiting substance (MIS), also known as anti-Müllerian hormone (AMH), has long been appreciated for its role in sex differentiation and reproduction, and sensitive ELISAs measuring blood levels are used in fertility clinics around the world as a measure of ovarian reserve (1–6). MIS plays important roles in the development of the gonad and the differentiation of the urogenital ridge. In the male fetus, MIS produced by the developing testes causes regression of the Müllerian duct (7). In the female fetus, MIS may play a role in early follicle assembly in the gonad by primordial germ cells (not to be confused with primordial follicles), since mice overexpressing MIS are devoid of germ cells shortly after birth (8), and, similarly, ex vivo incubation of fetal ovaries with MIS results in the inhibition of follicle assembly (9). These data highlight a role of MIS during fetal development that is distinct from its regulatory role of folliculogenesis postnatally.

In the adult, MIS is produced predominantly by the cumulus (less so by the mural) granulosa cells of secondary and early antral follicles (10). The receptor, Misr2, is expressed both in granulosa cells of follicles and in the ovarian surface epithelium (11–15).

It remains unclear how some primordial follicles can stay dormant from birth well into adulthood and by what mechanism they are selected for activation. However, some studies suggest MIS may be an important gatekeeper of their recruitment. The default state of primordial follicles is skewed toward activation, as evidenced by both transgenic mouse models and in vitro ovarian culture experiments. Although MIS-knockout females were initially fertile (8), young mice were found to contain more preantral and small antral follicles, and the window of fertility was shortened. Mice over 1 y old were nearly completely depleted of primordial follicles, suggesting unregulated recruitment of primordial follicles into the growing pool (16). Similarly, ex vivo cultures of ovarian cortical section, which contain only primordial and primary follicles, undergo recruitment of all primordial follicles in the absence of endogenous inhibitory signals. When ovarian cortical sections are implanted in chicken embryos, which contain high levels of MIS, primordial follicle recruitment is reduced (17). In contrast, when ovaries from Misr2-knockout mice are implanted in the chicken embryos, the primordial follicles are recruited at a high rate, equivalent to wild-type ovaries implanted in gonadectomized chicks with no MIS (17). Similarly, in ovarian cultures from postnatal day 4 rats, a stage at which only primordial follicles are present, 50 ng/mL MIS was sufficient to inhibit, albeit modestly, the transition of primordial to primary follicles compared with controls (18).

Until recently production of recombinant human MIS (rhMIS) protein was complicated by the low rates of activating cleavage,

Significance

All current reversible hormonal contraceptives rely on modulating gonadotropins or sex steroids by acting on the hypothalamic–pituitary–gonadal axis. Primordial follicle activation, the first step of folliculogenesis, is independent of gonadotropins or steroids. In this study we show that Müllerian inhibiting substance (MIS) can completely block primordial follicle activation, representing a unique mechanism of contraception that spares the pool of quiescent primordial follicles (ovarian reserve). Chemotherapy is thought to cause the over-recruitment of primordial follicles. Here we show that treatment with MIS during cycles of carboplatin, doxorubicin, or cyclophosphamide can significantly protect the ovarian reserve in mice. Thus, MIS may provide a paradigm of a reversible contraceptive that could mitigate damage to the ovarian reserve associated with gonadotoxic chemotherapeutics.

Author contributions: M.K., G.G., P.K.D., and D.P. designed research; M.K., A.E.S., L.Z., H.D.S., N.N., and D.P. performed research; D.W. and G.G. contributed new reagents/analytic tools; M.K., M.E.S., P.K.D., and D.P. analyzed data; and M.K., M.E.S., P.K.D., and D.P. wrote the paper.

Reviewers: R.N.F., Brown University; B.D.M., Université de Montréal; and T.K.W., Northwestern University.

The authors declare no conflict of interest.

Freely available online through the PNAS open access option.

See Commentary on page 2101.

[1]To whom correspondence may be addressed. Email: DPEPIN@mgh.harvard.edu or pdonahoe@partners.org.

This article contains supporting information online at www.pnas.org/lookup/suppl/doi:10.1073/pnas.1620729114/-/DCSupplemental.

low expression, and high rates of unwanted secondary cleavage contributing to a heterogeneous product (19, 20). To address these concerns, we created a cDNA construct (21) in which we replaced the **L**eader sequence with that of albumin and introduced a Q425**R** substitution in the C-terminal cleavage site to produce an MIS protein analog (**LR**-MIS, which we will refer to simply as "rhMIS"), with increased activating cleavage and secretion. The LR-MIS transgene also was used to produce an optimized adeno-associated virus serotype 9 (AAV9) gene therapy vector compatible with in vivo use, which we will refer to as "AAV9-MIS" (22).

Unlike other female contraceptive agents, which target more mature follicles by interfering with the hypothalamic–pituitary–gonadal axis [through modulation of 17β-estradiol (E2), progesterone (P4), luteinizing hormone (LH), follicle-stimulating hormone (FSH), and gonadotropin-releasing hormone (GnRH) feedbacks] to inhibit ovulation, MIS acts directly on the first step of folliculogenesis, primordial follicle recruitment, which occurs acyclically from birth (23–25). Controlling this rate-limiting step has important implications for primary ovarian insufficiency (POI), a condition characterized by an early onset of menopause and a catastrophic loss of ovarian reserve (26). One of the significant causes of POI is chemotherapy. Chemotherapy, particularly for childhood cancers (27, 28) and for cancers that affect women of reproductive age such as breast cancer (29), can have lasting effects on female fertility. In the breast cancer population alone in the United States the NIH estimates 246,660 women were diagnosed with breast cancer in 2016, of which 10.7% were under age 45, and a majority of which received potentially fertility-impairing treatments consisting of regimens of chemotherapy that include alkylating agents, doxorubicin (DOX), and taxanes (29). From this growing medical need was born the new field of oncofertility, which is devoted to the preservation of fertility in cancer patients (30, 31).

There are two ways by which chemotherapy is thought to damage the ovary: direct toxicity to follicles and indirect depletion of primordial follicles by over-recruitment (26). The latter is thought to occur as a consequence of the loss of negative feedback normally provided by growing follicles, which are highly susceptible to chemotherapeutic agents targeting proliferative cells (26).

Ovarian suppression has been proposed as a therapeutic modality for the preservation of the ovarian reserve (32). However, strategies to date have focused on GnRH inhibition, which has had limited success (33–35), likely because gonadotropins regulate only the late, irreversible stages of follicular maturation rather than the recruitment of primordial follicles (36). By directly inhibiting primordial follicle activation, we hypothesize that MIS could provide a unique method of contraception and a therapeutic option for oncofertility. MIS is an ideal biologic for this purpose; its safety profile is benign, given that its function in adults is predominantly restricted to the gonads, and MIS concentrations in baby boys (50–500 ng/mL) (37) and in patients with sex cord stromal tumors (3 μg/mL) (38) exceed those expected to affect folliculogenesis.

Results

MIS Administered as Gene Therapy or Purified Recombinant Protein Can Induce Superphysiological Blood Concentrations Sufficient to Act on Primordial Follicles of the Ovary. The availability of a biologically active rhMIS protein that can be produced and purified to high yields using chinese hamster ovary (CHO) cells (21) allowed us to explore higher and longer dosing in vivo, which previously had been impractical with the lower-cleavage wild-type protein (39) or impossible using commercial C-terminal recombinant MIS protein (R&D Systems, Inc.), which we found to be devoid of activity. For example, incubation of fetal [embryonic day (E)14.5] female rat urogenital ridges with 5 μg/mL of rhMIS for 72 h in ex vivo cultures causes nearly complete regression of the Müllerian duct (Fig. 1*A*, *Top Row*, *Right*), whereas the R&D Systems C-terminal MIS has no observable activity on the Müllerian duct bioassay (Fig. 1*A*, *Bottom Right*), the gold standard to test potency and specificity of the hormone (40). The rhMIS protein can be administered s.c. (Fig. 1*B*), i.v. (Fig. 1*C*), or i.p. (Fig. 1*D*), each resulting in a half-life of ∼4 h and reaching peak concentrations at 4 h, 30 min, and 2 h, respectively ($n = 3$ per group). The preferred route of delivery for rhMIS protein, when injected, was s.c., because its absorption kinetics were the most favorable. However, when osmotic pumps were used, i.p. implantation was found to be optimal and less prone to clogging, producing steady delivery for up to 1 wk (Fig. 1*E*) ($n = 3$). rhMIS activity was remarkably stable, with the material recovered from pumps that had been implanted in mice for 1 wk conserving full biological activity in the rat urogenital ridge bioassay (Fig. 1*A*, *Middle Row*, *Right*) (representative of $n = 3$).

Alternatively, a single i.p. administration of an AAV9 gene therapy vector (at 3e11 particles per mouse), which we have previously shown to induce persistent expression of the transgene for more than 1 y (22), efficiently delivers the rhMIS transgene to the liver, muscles, and pancreas of adult C57BL/6N mice (Fig. 1*G*) but not to the ovary (Fig. S1*A*). The resulting secreted rhMIS protein can be found at high concentrations (>0.25 μg/mL) in the blood as early as 2 d after injection when using an ELISA specific to the human protein (Fig. 1*F*) ($n = 3$).

With delivery of MIS optimized, we could evaluate the inhibitory activity of MIS on the recruitment of ovarian primordial follicles in vivo. We confirmed that *Misr2* was expressed by granulosa cells at all early stages of folliculogenesis, including primordial follicles (Fig. S2*A*), with their germ cells identifiable by immunofluorescence (IF) based on their $P63^+$ nucleus and mouse vasa homolog $(Mvh)^+$ cytoplasm (a representative example is shown in the inset of Fig. S2*A*).

AAV9-MIS Treatment Results in Reversible Ovarian Quiescence. A single i.p. administration of AAV9-MIS vector in adult (6- to 7-wk-old) female Nu/Nu mice induces a viral titer-dependent increase in circulating MIS (Fig. S2 *B* and *C*), which can be detected by an ELISA specific to the human protein (2, 21). The circulating level of rhMIS was remarkably stable over the 60 d of the experiment (Fig. S2*C*); 1e12 particles generated serum concentrations from 1.5 to 2.7 μg/mL; 3e11 particles generated concentrations of 0.8–2 μg/mL; 1e11 particles generated concentrations of 0.2–0.7 μg/mL; 1e10 particles generated concentrations of 1–17 ng/mL; and the AAV9-GFP control had no detectable human MIS protein. Mice treated with doses of 1e11 or more AAV9-MIS viral particles had a marked reduction in growing follicles (Fig. S2*B*). We chose the middle dose of 3e11 for subsequent experiments. Ovaries from mice treated with 3e11 particles of AAV9-MIS and euthanized 39 d later were visibly smaller than ovaries from control mice treated with AAV9-GFP (Fig. 2*A*) as a consequence of the profound reduction in growing follicles evidenced in the representative (of $n = 3$) middle sections of the ovaries (Fig. 2*B*). The reduced ovarian size was observed in mice treated for 1–2 mo, but not earlier, suggesting gradual depletion of developing follicles. Ovaries harvested 39 d after treatment from three control females treated with AAV9-GFP and three females treated with AAV9-MIS were sectioned in their entirety, and total follicle counts were performed (Fig. 2*C*). The AAV9-MIS ovaries were almost completely devoid of growing follicles, with marked reductions of primary follicles (−65%; $P < 0.001$), secondary follicles (−96%; $P < 0.001$), and antral follicles (−97%; $P < 0.001$) (Fig. 2*C*). Interestingly, this reduction is unlikely to be caused by germ cell toxicity or enhanced large follicle atresia, because primordial follicle counts were unchanged, and atretic follicles actually were significantly reduced compared with control ovaries (−88%; $P < 0.001$) (Fig. 2*C*), as is consistent with a blockade of primordial follicle activation.

To test if the primordial follicle inhibition is reversible, C57BL6/N mice were treated with AAV9-MIS and were allowed to deplete their

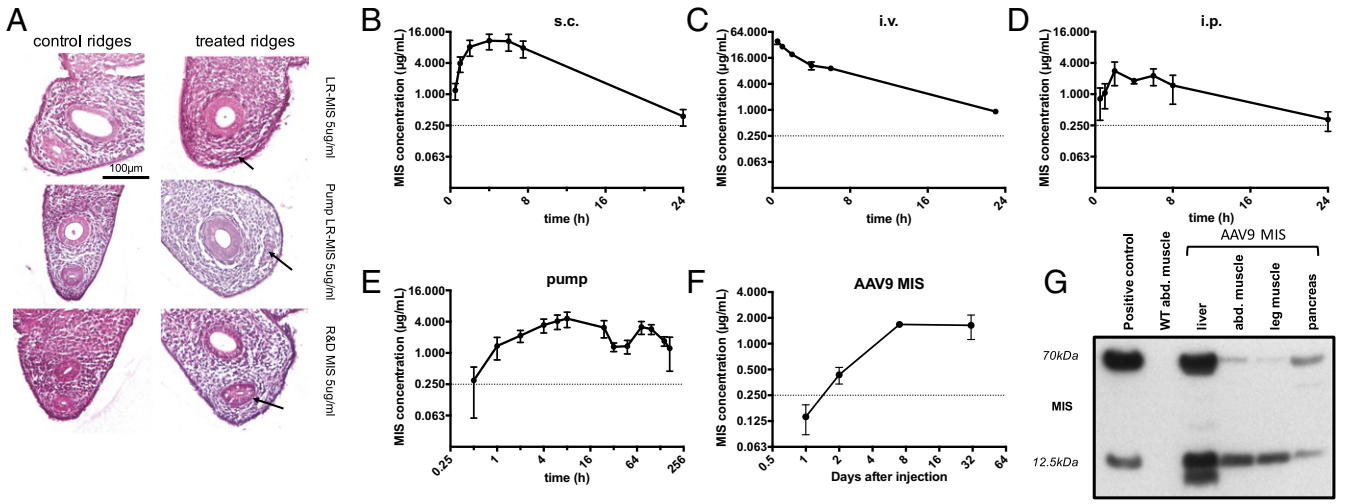


Fig. 1. Comparative analysis of multiple modes of MIS administration. (*A*) Rat fetal (E14.5) urogenital ridges were incubated ex vivo with recombinant protein (*Right*), and the contralateral ridge was mock-treated (*Left*) for 72 h. Shown are representative sections from ridges treated with fresh rhMIS (LR-MIS) protein at 5 μg/mL (*Top*), rhMIS recovered from a pump implanted for 1 wk in a mouse at 5 μg/mL (*Middle*), or commercially obtained (R&D Systems) C-terminal MIS protein produced in *Escherichia coli* at 5 μg/mL (*Bottom*). Regressed (*Top* and *Middle*) or intact (*Bottom*) Müllerian ducts are indicated by arrows. (*B*–*F*) Pharmacokinetics of MIS administered by different delivery routes with serum levels of MIS measured serially with a human-specific ELISA. (*B*) Bolus injection, 3 mg/kg s.c. ($n = 3$). (*C*) Bolus injection, 3 mg/kg i.v. ($n = 3$). (*D*) Bolus injection, 1.5 mg/kg i.p. ($n = 3$). (*E*) Implanted i.p. osmotic pump delivering rhMIS at a rate of 0.6 μg/h. (*F*) AAV9-MIS 3e11 particles per mouse ($n = 5$). (*G*) A representative Western blot of MIS protein showing the prohormone (70 kDa) and cleaved C-terminal (12.5 kDa) peptide from tissue protein lysates of a mouse injected with 3e11 particles of AAV9-MIS. Controls include CHO-K1–LR-MIS–conditioned medium as a positive control and lysate from uninjected (WT) muscle protein as a negative control.

pool of growing follicles for 60 d, after which their ovaries were transplanted orthotopically into the unilaterally gonadectomized bursa of either AAV9-GFP– or AAV9-MIS–treated recipient female mice (Fig. 2*D*). Folliculogenesis was "reawakened," with visible secondary and antral follicles as early as 12 d after quiescent ovaries were transplanted into AAV9-GFP recipients that did not have superphysiological levels of MIS, whereas the ovaries remain dormant when reintroduced into another AAV9-MIS–treated recipient as a transplantation control (Fig. 2*E*).

Treatment with rhMIS Protein Results in Reversible Ovarian Quiescence. To confirm that the inhibition of primordial follicle activation is not a unique property of gene therapy delivery and to elucidate the kinetics of ovarian reawakening, we tested the effect of parenteral treatment with rhMIS protein in Nu/Nu mice. The protein was administered s.c. twice daily (every 12 h), at a dosage of 1.5 mg/kg (Fig. 3*A*, *Upper*), which *in silico* pharmacokinetic modeling predicted would maintain circulating levels of rhMIS above our target level of 0.25 μg/mL (Fig. 3*D*) (the lower range achieved using 1e11 AAV9-MIS) (Fig. S2*C*). Actual circulating levels of rhMIS measured by ELISA 12 h after injection, representing the trough, were maintained above the target threshold of 0.25 μg/mL (Fig. 3*C*), as predicted by *in silico* simulations of pharmacokinetics (Fig. 3*D*). Ovaries from rhMIS-treated mice were markedly reduced in size, as evidenced by a representative (of $n = 3$) middle section following 40 d of treatment, thus phenocopying the treatment with AAV9-MIS (Fig. 3 *A* and *B*). As expected, ovaries from rhMIS-treated mice contained fewer primary, secondary, and antral follicles than ovaries from saline-treated controls (Fig. 3*B*). As ovaries were released from quiescence following cessation of treatment with rhMIS protein, folliculogenesis resumed (Fig. S3). We observed a trend for a rapid increase in primary follicles from day 0 to day 5 posttreatment, followed by a plateau at a level comparable to the counts seen in normally cycling saline-treated control mice (Fig. 3*B*). There was a significant increase ($P = 0.0002$) in secondary follicles from day 5 to day 10 and a trend for a continued increase from day 10 to day 15 to levels equivalent those into saline-treated controls. However, the number of antral follicles did not rise significantly to levels comparable to those in saline-treated controls within the short time frame of this experiment (Fig. 3*B*). There also was a trend for a reduction in primordial follicles following reawakening, suggesting some overactivation (Fig. 3*B*). The timing of reactivation was consistent with the appearance of growing follicles at day 12 in the AAV9 transplantation experiment (Fig. 2*E*).

Gene Therapy with AAV9-MIS as a Vectored Contraceptive. To evaluate the effectiveness of MIS as a contraceptive, we tested the effects of AAV9-MIS treatment on C57BL/6N mice and examined various fertility end points. The estrus cycle of mice treated with AAV9-MIS ($n = 3$) and mice treated with AAV9 empty control ($n = 3$) were monitored by daily vaginal swabs. After an initial period of regular cycling in the 35 d following injection of the virus, the cycle of AAV9-MIS–treated mice became irregular at week 5 (Fig. 4*A*), with significantly ($P = 0.0004$) more time spent in apparent estrus from day 36–70 (Fig. 4*B*). The vaginal swabs of acyclic mice (Fig. S2 *E* and *F*) resembled the estrus-like cytology typical of ovarian insufficiency (41), which presents as cornified epithelium and should not be confused with the true estrus of cycling mice (42). Female C57BL/6N mice treated with AAV9-MIS ($n = 10$) or AAV9 empty control ($n = 10$) were paired with proven male breeders 3 d after AAV9 injection and were mated continuously for 6 mo. Consistent with the gradual depletion of growing follicles, the two groups of females had litters of similar size for their initial litters produced within the first 6-wk interval immediately following injection (Fig. 4*C*). Interestingly, litters born during this time to mothers with high levels of MIS had normal sex ratios, normal Müllerian duct development, and no detectable MIS in their blood, suggesting that the protein does not cross the placental barrier or affect the mother's pregnancy. For the analysis of fertility, we grouped mice that experienced any period of circulating levels of MIS below our target threshold of 0.25 μg/mL as "AAV9-MIS low" ($n = 4$) and those that maintained MIS levels above the 0.25μg/mL threshold as "AAV9-MIS high" ($n = 6$) (Fig. 4*D*). AAV9-MIS high mice became completely infertile after 6 wk, whereas AAV9-MIS low mice experienced reduced fertility,

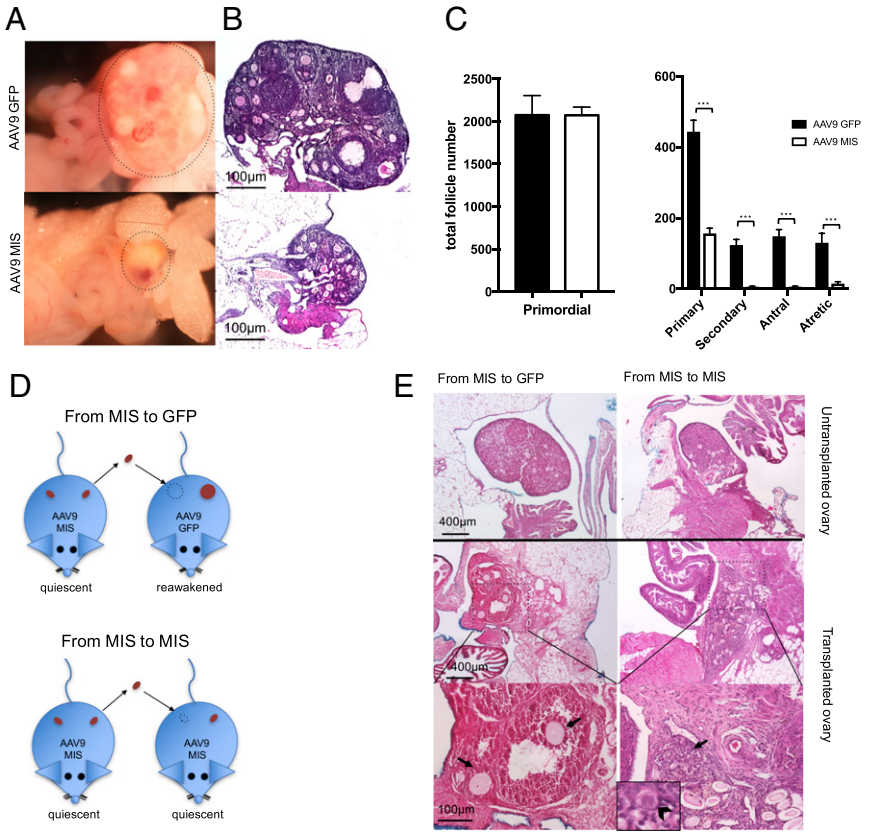


Fig. 2. AAV9-MIS treatment results in reversible ovarian quiescence. Mice were treated with a single dose of AAV9-MIS at 3e11 particles per mouse, and ovaries were examined after 39 d. (*A*) Representative gross morphology (ovary circled with dashed line). (*B*) A representative middle section compared with an AAV9-GFP control ovary. (*C*) Total follicle counts in AAV9-MIS and AAV9-GFP mice 39 d after treatment with a single dose of 3e11 viral particles ($n = 5$ mice per group). ***$P < 0.001$ by Student's t test. (*D*) Schematic for the transplantation of ovaries from mice treated with AAV9-MIS for 60 d into AAV9-GFP or AAV9-MIS recipients. (*E*) Representative intact contralateral ovaries (*Top*) or middle sections from transplanted ovaries ($n = 5$) (*Middle*) from two donor mice pretreated with AAV9-MIS, transplanted 60 d later into AAV9-GFP or AAV9-MIS recipients, and recovered 12 d after transplantation. (*Bottom*, *Left*) Higher-magnification image of growing follicles indicated by arrows. (*Bottom*, *Right*) Quiescent primordial follicles indicated by arrowhead. (*Inset* magnification: 400×.)

producing a few small litters during the course of the mating experiment (Fig. 4*C*). Cumulative numbers of litters per female were reduced significantly in both the high ($P < 0.0001$) and low ($P < 0.0001$) groups (Fig. 4*C*). When the same females were mated for 1 mo at 1 y of age, control females still had some residual fertility, producing an average of one pup per female, whereas all the treated females remained infertile ($P = 0.0065$) (Fig. S2*D*). Following the 6-mo mating study (between days 232 and 309), blood samples were taken at estrus, as determined by vaginal cytology, from both treated and control female mice to assess reproductive hormone levels. As predicted by the depletion of early-growing follicles, there was a significant reduction in inhibinB (InhB) ($P = 0.0024$), E2 ($P = 0.0026$), and its precursor testosterone ($P = 0.0093$) in mice treated with AAV9-MIS compared with controls; however, P4 levels were unaffected (Fig. 4*E*). As expected from pituitary feedback, gonadotropins were elevated, with trends for greater FSH and LH levels in females treated with AAV9-MIS than in controls (Fig. 4*E*) (43).

MIS Treatment Reduces Primordial Follicle Depletion Induced by Chemotherapy. To evaluate ovarian suppression by MIS as a protective therapy against chemotherapy-induced ovarian reserve depletion, we tested both the AAV9-MIS gene therapy and the rhMIS protein in mouse models treated with chemotherapy. For this purpose we administered AAV9-MIS or AAV9-GFP to adult (6- to 7-wk-old) tumor-bearing Nu/Nu mice and 1 d later began weekly doses of carboplatin (CBP) ($n = 10$) at 80 mg/kg i.p. or DOX ($n = 9$) at 3 mg/kg i.v. until the mice were euthanized for tumor-related end points (volume >1 cm^3) at days 10 and 12, respectively (Fig. 5*A*). Tumor growth in this short timespan was not affected by MIS. Ovaries were retrieved and serially sectioned, and total follicle counts were performed. We observed significantly higher ovarian reserves in mice cotreated with AAV9-MIS than in control mice treated with AAV9-GFP, with primordial follicle counts 2.2-fold higher ($P < 0.001$) in CBP-treated mice and 1.8-fold higher ($P < 0.01$) in the DOX-treated mice (Fig. 5 *B* and *C*). No differences were observed in growing follicle counts; however, using immunohistochemistry (IHC), we noticed an abundance of growing follicles with extensive granulosa cell apoptosis, as evidenced by pycnotic hematoxylin staining and cleaved caspase-3 staining in all groups (Fig. S2 *G* and *H*). We did not find cleaved caspase-3^+ primordial follicles.

To test the efficacy of rhMIS protein for the preservation of ovarian reserve, we elected to use osmotic pumps implanted i.p. in C57BL/6N female mice to allow very precise delivery of MIS (Fig. 1*E*). In this model we implanted osmotic pumps loaded with 100 μL of a 1,200-μg/mL solution of rhMIS diluted in saline or saline-loaded control pumps, which were replaced every 7 or 5 d (Fig. 5*D*). The day after pump implantation, mice began a weekly treatment of i.p. chemotherapy or saline control, using doses of 60 mg/kg for CBP, 7.5 mg/kg for DOX, and 60 mg/kg for cyclophosphamide (CPA) (Fig. 5 *E*–*G*). After 2 wk of chemotherapy, mice were euthanized, ovaries were retrieved and serially sectioned, and total follicle counts were performed. We observed significantly higher ovarian reserves in mice that had been implanted with rhMIS-eluting pumps before receiving chemotherapy than in controls that had been implanted with saline pumps and that received the same chemotherapy. Primordial follicle counts were 1.4-fold higher ($P < 0.0001$) in CBP-treated mice, 2.9-fold higher ($P < 0.001$) in DOX-treated mice, and 1.2-fold higher ($P < 0.05$) in CPA-treated mice (Fig. 5 *E*–*G*). Treatment with rhMIS alone did not significantly affect either primordial or growing follicles within this short timespan; however, there was a trend toward lower numbers of growing follicles compared with saline-only controls (Fig. 5 *E*–*G*). Using an ELISA capable of detecting the murine protein (Fig. S1*B*), we found that treatment with chemotherapy alone produced a trend for decreased endogenous mouse MIS when the blood from the same mice was compared pre- and postchemotherapy (at the 14-d time point), and the decrease achieved statistical significance with CPA treatment ($P = 0.015$) (Fig. S1*A*).

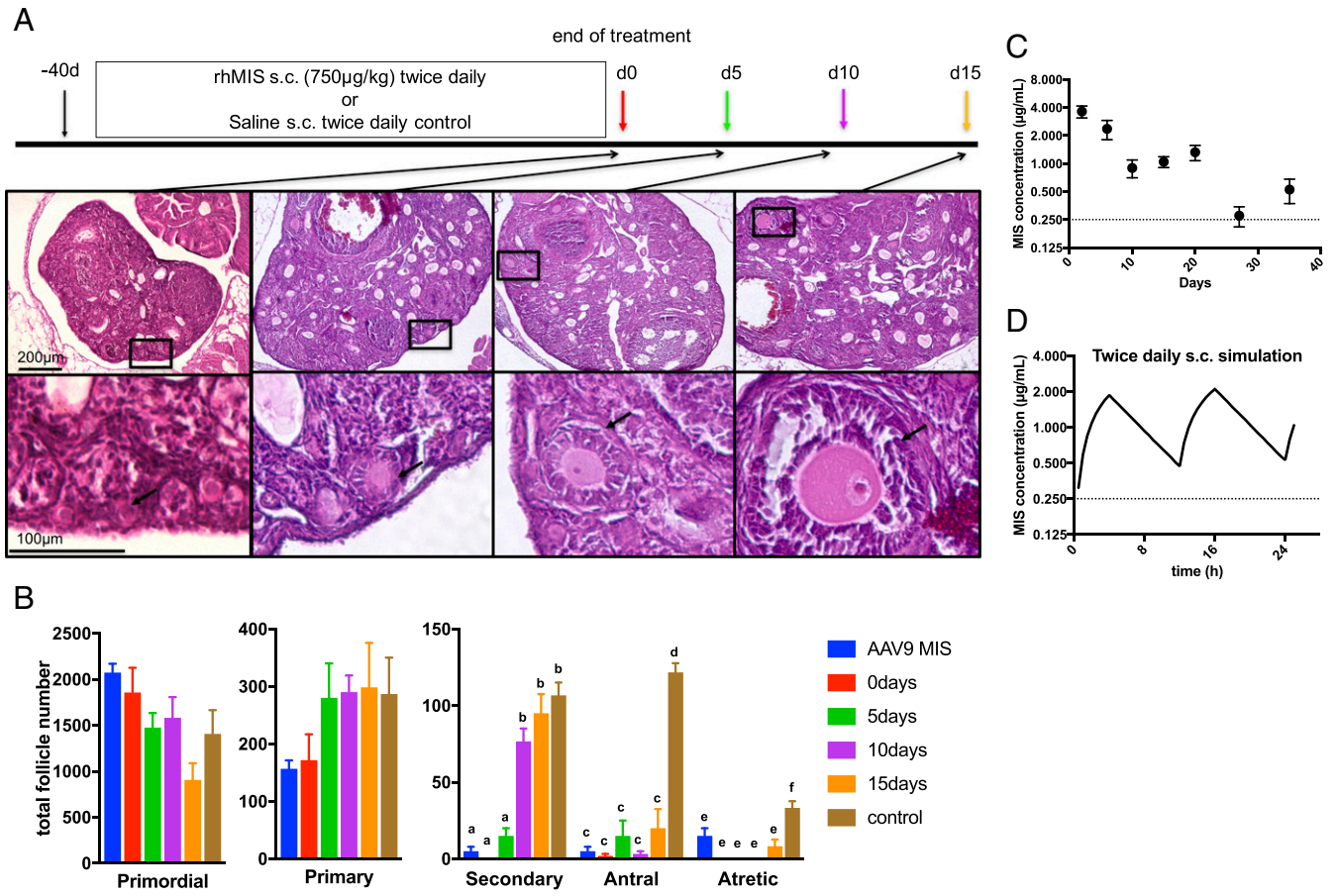


Fig. 3. Treatment with rhMIS protein results in reversible ovarian quiescence. (*A*) Mice were treated twice daily (every 12 h) with an s.c. injection of 750 μg/kg of rhMIS for 40 consecutive days and were euthanized at days 0, 5, 10, and 15 posttreatment. Shown are representative middle sections from ovaries of mice at days 0, 5, 10, and 15 posttreatment (*Upper Row*, *Left to Right*) and higher-magnification examples of quiescent primordial (*Lower Row*, *Left Image*) or growing (*Lower Row*, *Three Right Images*) follicles. (*B*) Total follicle counts from ovaries of mice treated for 40 d with rhMIS protein and released for 0, 5, 10, or 15 d and controls consisting of AAV9-MIS as a positive control of complete quiescence (*Left*), or saline as a negative control with normal folliculogenesis (*Right*, control). Different letters (a–f) above the bars indicate significance ($P < 0.05$) within each category of follicle by one-way ANOVA. (*C*) Serum MIS levels as measured by ELISA during the 40 d of s.c. treatment with 1.5 mg/kg of rhMIS protein, taken at the trough (12 h after injection). (*D*) Simulation of the pharmacokinetics of s.c. administration of 1.5 mg/kg of rhMIS protein every 12 h over a 24-h interval.

Discussion

The MIS receptor *Misr2* has long been known to be expressed by ovarian surface epithelium and granulosa cells of the ovary (11), and its promoter is often used in the generation of conditional transgenic mice for these cell types (44) and in mouse models of gynecological cancers (15). Our results confirm that *Misr2* expression during folliculogenesis may begin as early as the primordial stage and may persist from birth until the depletion of those follicles (Fig. S2*A*). Reports of the effect of MIS on follicles have been mixed, with some studies suggesting an activating effect (45, 46) and others implying a direct inhibitory effect (18, 47), indirect inhibition via gonadotropins (48, 49), or even regulation of meiosis (50). In past studies, the magnitude of inhibition of primordial follicle recruitment in vivo and in vitro has been perceived as relatively modest because of difficulties in achieving high concentrations of the protein. With tools such as the rhMIS analog LR-MIS (21) and the use of gene therapy vectors such as AAV9 (22), we have been able to test the effects of high (perhaps superphysiological) levels of MIS on the ovaries of adult mice. The local concentration of MIS in the mouse ovarian cortex, where primordial follicles reside, is unknown. However, in humans the concentration of MIS in the follicular fluid of small antral follicles is greater than 1 μg/mL, i.e., three orders of magnitude higher than the serum levels (51), suggesting that primordial follicles may be exposed to levels of MIS in excess of serum concentration. In contrast to previous studies, we find MIS is capable of inducing a complete shutdown of folliculogenesis when maintained at levels over 0.25 μg/mL in the blood in two different strains of mice: C57BL/6N and Nu/Nu (the latter ruling out any major effect of immunogenicity of the human protein). Follicle counts suggest a specific inhibition of primordial follicle activation without inhibition or activation of other stages or increases in the rate of atresia (see the two columns at the far right in Fig. 2*C*, *Right*). Consistent with this hypothesis, the MIS-induced ovarian quiescence takes ∼5 wk to manifest, as seen by cycling and mating studies (Fig. 4 *A* and *C*), suggesting the already growing follicles complete their irreversible development and are gradually depleted from the ovary (Fig. S3). Furthermore, that both the estrus cycle and the fertility of MIS-treated mice during the first 5 wk of treatment are not different from controls suggests that any positive or negative effect of MIS on other stages of folliculogenesis or gonadotropin/steroid levels is biologically insignificant for fertility. Furthermore, the results of many studies using commercial C-terminal MIS protein in the context of fertility should be interpreted with caution, given that peptide's lack of specific biological activity in the rat fetal urogenital ridge bioassay (Fig. 1*A*).

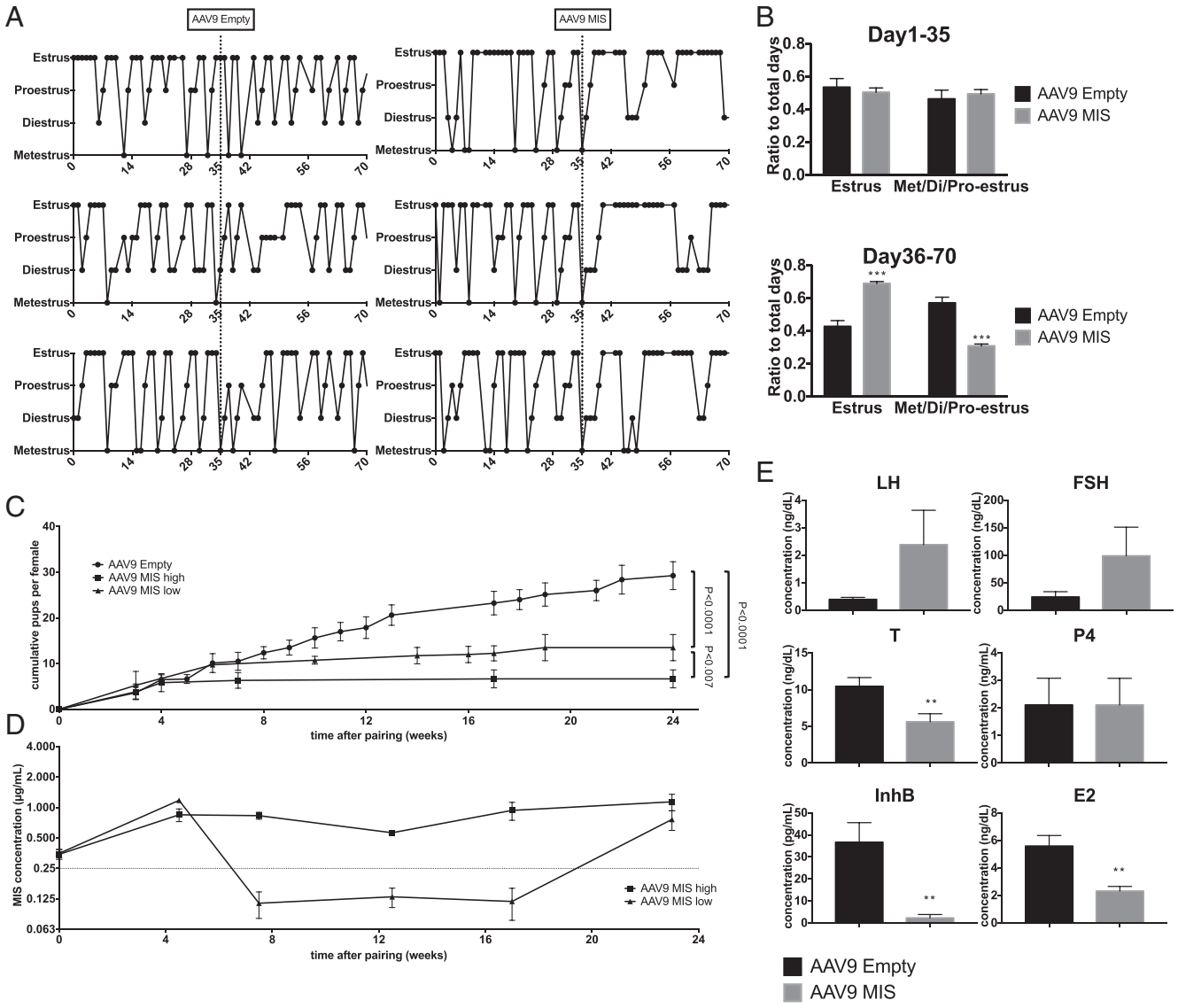


Fig. 4. Treatment with AAV9-MIS results in a progressive loss of cycling and fertility and the induction of a hypergonadotropic hypogonadic hormonal profile. (*A*) Mice were treated with a single injection of 3e11 particles of AAV9-MIS or AAV9-empty vector control, and cycling was monitored by daily vaginal swabs over 70 d. (*B*) The relative amount of time spent in estrus was compared for the first half (day 1–day 35) and the second half (day 36–day 70) of the observation period in both groups. (*C*) Mating trios ($n = 10$ trios) consisting of a proven male breeder with an AAV9-MIS and an AAV9-empty vector control female were housed together continuously for a 6-mo interval, and the average cumulative number of pups per female was compared by ANOVA with a Holm–Sidak post hoc test (*P* values are indicated). (*D*) Females treated with AAV9-MIS were split into two groups, AAV9-MIS high and low, based whether their serum levels of MIS, as measured by ELISA, were above or below the 0.25 μg/mL threshold for the duration of the experiment. (*E*) Following the 6-mo breeding experiment, serum samples were collected, and the levels of LH, FSH, testosterone (T), P4, InhB, and E2 were measured by ELISA. $^{**}P < 0.01$ and $^{***}P < 0.001$ by Student's *t* test.

Remarkably, the inhibition of primordial follicle activation by MIS was found to be reversible with ovarian transplantation from AAV9-treated animals and in short-term protein treatment experiments (Figs. 2*E* and 3). The reawakening of folliculogenesis was rapid (Fig. S3, model), with the number of secondary follicles gradually recovering to within the normal range 15 d after the cessation of treatment with the rhMIS protein (Fig. 3*B*). This dramatic activation of primordial follicles and quick maturation to the secondary stage may be accelerated by the absence of feedback from growing follicles and the resulting reduced endogenous MIS and elevated gonadotropins (Fig. 4*E*). Therefore, careful weaning from exogenous MIS may be necessary to avoid overactivation of primordial follicles following treatment. Prolonged treatment with MIS and the corresponding depletion of growing follicles also decreased E2, testosterone, and InhB levels and increased gonadotropin levels (Fig. 4*E*). The induced hypergonadotropic hypogonadism was associated with disrupted estrus cycling and persistent vaginal cornification (Fig. 4*A* and Fig. S2 *E* and *F*) (42).

Given the nearly complete blocking of folliculogenesis and the resulting infertility of treated mice (Fig. 4*C*), MIS or agonists targeting its pathway may represent a unique hormonal contraceptive approach. Unlike current hormonal contraceptives that disrupt the hypothalamus–pituitary–gonadal axis and act on already committed secondary and antral follicles, MIS inhibits the first step of activation of the dormant primordial follicle, potentially sparing the germ cell. It has not escaped our notice that

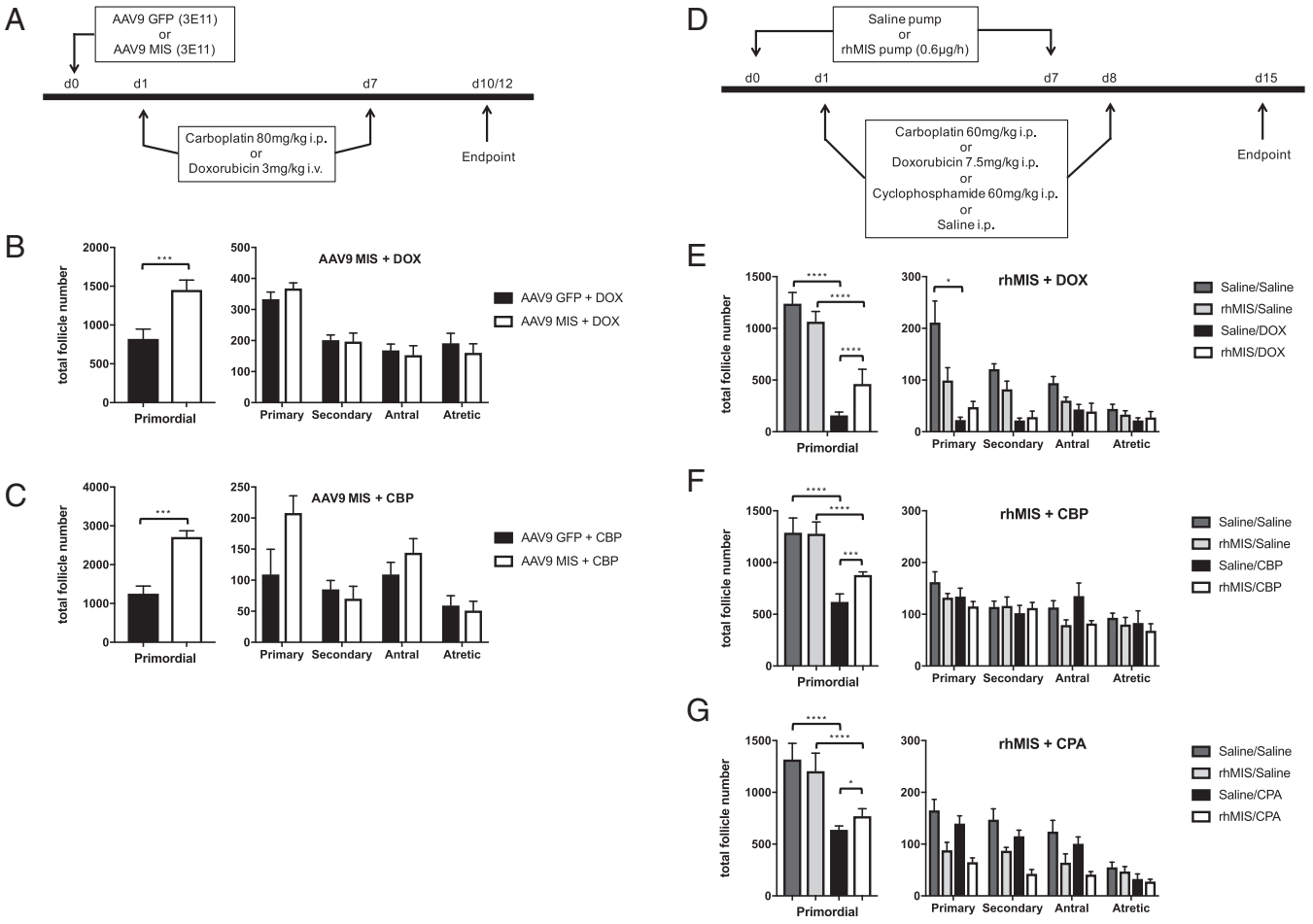


Fig. 5. Treatment with MIS protects the ovarian reserve from the primordial follicle depletion induced by chemotherapy. (*A*) Mice were treated with a single injection of 3e11 particles of AAV9-MIS or AAV9-GFP control, and weekly chemotherapy started 1 d later. Mice were euthanized either 3 d (DOX) or 5 d (CBP) after the second chemotherapeutic injection. (*B* and *C*) Total follicle counts were performed for AAV9-MIS ($n = 5$) and AAV9-GFP ($n = 5$) mice treated with 80 mg/kg CBP i.p. (*B*) or 3 mg/kg DOX i.v. (*C*) and were analyzed by Student's *t* test. (*D*) Mice were implanted i.p. with pumps delivering either rhMIS protein at 0.6 µg/h or saline as a negative control. Pumps were replaced every 5 or 7 d. Weekly rounds of chemotherapy were started 1 d after implantation of the pump. Mice were euthanized 1 wk after the last dose of chemotherapy. (*E–G*) Total follicle counts were performed for saline pump + saline i.p. controls, rhMIS protein pump + saline i.p. controls, saline pump + chemotherapy i.p., and rhMIS protein pump + chemotherapy i.p. ($n = 5$ per group) for (*E*) DOX 7.5 mg/kg i.p., (*F*) CBP 60 mg/kg i.p., and (*G*) CPA 60 mg/kg i.p. Average follicle counts were analyzed by two-way ANOVA with a Holm–Sidak post hoc test; $*P < 0.05$, $***P < 0.001$, and $****P < 0.0001$.

the chronic use of a contraceptive method sparing germ cells suggests the possibility of extending the reproductive lifespan of the user; however, matters of oocyte quality associated with aging remain to be resolved. More practically, vectored contraceptives using MIS may be very useful in the veterinary setting where a single injection could be used as a permanent contraceptive for female cats and dogs in temporary shelter, because AAVs are not replication competent and have a history of safe use for that purpose (52).

The unique specificity and mechanism of action of MIS present some therapeutic opportunities not afforded by current hormonal contraceptives. Limiting primordial follicle activation could lessen the premature depletion of the ovarian reserve observed in cases of POI induced by environmental, iatrogenic, or genetic causes. This is particularly true in cases where POI may be exacerbated by primordial follicle over-recruitment, i.e., in which specific toxicities to growing follicles increase the activation rate of primordial follicles (26). We hypothesize that secondary primordial follicle depletion may result from the reduction in endogenous MIS, which normally is secreted by granulosa cells of growing follicles and provides negative feedback to the primordial follicle (Fig. 6, model); MIS levels are also known to decline during chemotherapy (53). We further hypothesize that this deficit could be addressed directly by supplementing exogenous MIS, as a form of hormone replacement therapy, to restore this negative feedback (Fig.6, model). To test these hypotheses, we used gene therapy with MIS, or rhMIS parenteral protein administration, to create a complete arrest in primordial follicle activation concurrently with chemotherapy cycles. As a proof of concept we chose three commonly used chemotherapeutic classes with well-described gonadotoxicities: platinums (54), anthracyclins (55), and alkylating agents (56). Both platinums (such as CBP) and anthracyclins (DOX) interfere with DNA replication and as such are particularly toxic to dividing granulosa cells of secondary and antral follicles, albeit with distinct toxicity profiles (55), and thus represent ideal targets for an MIS oncofertility intervention. CPA is an alkylating agent, a class that is particularly damaging to germ cells, and is the most problematic gonadotoxic chemotherapeutic in the clinic, particularly because it is often used in young girls with hematological cancers (57). We found that MIS had a particularly dramatic protective effect in the case of DNA-damaging agents (Fig. 5 *B*, *C*, *E*, and *F*) but was only weakly protective for CPA (Fig. 5*G*). We speculate that the degree of protection likely

reflects the relative amounts of direct damage to the germ cells versus the indirect damage caused by the loss of negative feedback and over-recruitment of primordial follicles. A recent investigation on the relative contribution of the direct versus indirect damage caused by various chemotherapeutics demonstrated that, although some agents, such as CPA have greater toxicity to germ cells of quiescent primordial follicles, others, such as gemcitabine, leave them relatively unscathed, instead causing cell death in the dividing granulosa cells of growing follicles. We predict MIS treatment would be most suitable in the latter case (58).

Treatment with MIS is particularly compatible with short-term oncofertility use such as during chemotherapy, because complete blockade of folliculogenesis induces a menopausal-like state of acyclicity and hypergonadotropic hypogonadism (Fig. 4*E*). In some cases, such as breast cancer, reduced estradiol is considered beneficial to the treatment of the tumor (29); thus ovarian suppression might offer an additional advantage in these instances. Additionally, for conditions such as polycystic ovarian syndrome (59), the reduction of both folliculogenesis and androgens observed with MIS may alleviate some of the most important symptoms. However, in other contexts, chronic long-term use of MIS as a contraceptive likely would have to be associated with steroid hormone replacement therapy. Alternatively, one could envision the use of a lower dosage of MIS with which primordial follicle activation could be partially reduced but not completely inhibited, thus slowing the depletion of the ovarian reserve in patients with diminished ovarian reserve such as carriers of the fragile X mental retardation 1 premutation (60). Finally, another application in which MIS may be useful is in the treatment of primordial follicle depletion associated with ovarian tissue grafting (61), an experimental fertility-preservation technique in which cortical ovarian grafts are frozen and reimplanted after chemotherapy (62). The relatively modest lifespan of such grafts could be expanded if the initial primordial follicle loss upon reimplantation could be moderated.

In conclusion, we have demonstrated that MIS is a potent inhibitor of primordial follicle activation and is an effective contraceptive in mice. Its unique mechanism of action makes it particularly suited for the protection of ovarian reserve during chemotherapy and opens up many clinical possibilities in other conditions in which the recruitment of follicles is dysregulated. Future studies should address the quality of the eggs being preserved and evaluate ways to mitigate the long-term effects of hypergonadotropic hypogonadism.

Materials and Methods

Animals. This study was performed in accordance with experimental protocols 2009N000033 and 2014N000275 approved by the Massachusetts General Hospital Institutional Animal Care and Use Committee. Under those protocols, euthanasia was performed by CO_2 asphyxiation or by barbiturate overdose using a commercial preparation (sodium pentobarbital 390 mg + sodium phenytoin 50 mg/mL) (Euthasol) 0.22 mL/kg i.p. (86 mg/kg pentobarbital) respectively, in compliance with the *Guide for the Care and Use of Laboratory Animals* guideline (63).

For pharmacokinetic analysis, rhMIS protein was delivered to 6- to 7-wk-old C57BL/6N female mice (Charles River Laboratories) s.c. (3 mg/kg; $n = 3$), i.v. (3 mg/kg; $n = 3$), i.p. (1.5 mg/kg; $n = 3$), or by an i.p. implanted osmotic pump (ALZET 1007D, DURECT Corporation) with a flow rate of 0.5 μL/h, filled with 1,200 μg/mL of LR-MIS ($n = 3$). After the delivery of LR-MIS, blood samples were collected serially and analyzed.

To investigate the effect of AAV9-MIS on the ovaries, 6- to 7-wk-old Nu/Nu female mice (Massachusetts General Hospital) were injected i.p with 1e10, 1e11, 3e11, or 1e12 particles of AAV9-MIS ($n = 1$), and blood samples were collected serially. After 7 wk of treatment, the animals were euthanized, ovaries were dissected, and ovarian follicles were counted as described below.

To observe the effect of releasing ovaries from exogenous MIS ovarian suppression, 3e11 viral particles of AAV9-MIS were given i.p. to 6- to 7-wk-old C57BL/6N female mice; 60 d later one ovary per mouse was surgically transplanted orthotopically into the emptied bursa of either an AAV9-MIS–treated or an AAV9-GFP–treated female mouse. Mice were euthanized 12 d after the transplantation, and ovaries were dissected.

To see the effect of short-term rhMIS protein ovarian suppression, 6- to 7-wk-old Nu/Nu female mice were injected s.c. with 750 μg/kg of rhMIS every 12 h for 40 d. The mice were euthanized 0 ($n = 3$), 5 ($n = 3$), 10 ($n = 3$), or 15 ($n = 3$) d after the injections were stopped, and the ovaries were examined to assess the recovery of folliculogenesis.

Histology. Dissected ovaries were fixed in 4% (wt/vol) paraformaldehyde overnight at 4 °C and were embedded in paraffin blocks in an automated tissue processor (Leica TP1020). For H&E staining, the whole ovary was cut into 8-μm sections, and serial sections were mounted on slides and deparaffinized. After the graded series of rehydration, sections were stained with hematoxylin (Dako) and eosin (Sigma Aldrich), coverslipped with Cytoseal 60 (Thermo Fisher Scientific), and examined under the light microscope for follicle counts.

For IHC and IF, the ovaries were cut into 5-μm thicknesses and were mounted on slides. Slides were deparaffinized and rehydrated, and heat-induced antigen retrieval was performed.

For IHC, after endogenous peroxidase was inactivated by 3% (vol/vol) hydrogen peroxide (Thermo Fisher Scientific), sections were blocked in Tris-buffered saline and Tween20 (TBST) solution containing 2% (vol/vol) donkey serum (Jackson ImmunoResearch) and were incubated in primary antibody overnight at 4 °C. Then the sections were incubated in an HRP-conjugated secondary antibody for 1.5 h, and 3,3′-diaminobenzidine (DAB) (DAKO) was used to visualize the signal.

For IF, sections were blocked in 2% (vol/vol) donkey serum blocking buffer and were incubated in primary antibody overnight at 4 °C. Then the sections were incubated in secondary antibodies for 1.5 h and were coverslipped with VECTASHIELD mounting medium with DAPI (Vector Laboratories). The slides were examined 15 min after coverslipping under a Nikon Eclipse i80 microscope. Primary antibodies included sheep anti-hMISR2 polyclonal antibody (R&D Systems), rabbit anti-cleaved caspase-3 polyclonal antibody (Cell Signaling Technology), rabbit anti-MVH polyclonal antibody (Abcam), and mouse anti-p63 monoclonal antibody (Biocare Medical). Secondary antibodies included donkey anti-sheep IgG antibody conjugated to HRP (R&D Systems), donkey anti-rabbit IgG antibody conjugated to HRP (Jackson ImmunoResearch), Alexa Fluor 488-conjugated donkey anti-sheep IgG antibody, Alexa Fluor 555-conjugated donkey anti-rabbit IgG antibody, and Alexa Fluor 647-conjugated donkey anti-mouse IgG antibody (Thermo Fisher Scientific).

Follicle Counts. Follicle counts were performed blinded as previously described (64). Briefly, the total number of follicles in each ovary was estimated by counting the numbers of follicles in every fifth section of H&E-stained whole ovaries and applying a fivefold correction factor. Follicles were classified into five stages: primordial, primary, secondary, antral, and atretic follicles. Only follicles that had an oocyte nucleus were scored. Follicles whose oocyte was surrounded by a layer of squamous granulosa cells were classified as primordial follicles. If a single layer of cuboidal granulosa cells was observed, follicles were classified as primary follicles. Secondary follicles had multiple layers of cuboidal granulosa cells. If an antrum was observed in the granulosa cell layers, the follicle was classified as an antral follicle. Atretic follicles were counted only when an aberrant oocyte and multiple layers of pycnotic granulosa cells were observed. Follicle counts were performed in both ovaries of $n = 5$ mice per group for the experiment shown in Fig. 2*C*, $n = 3$

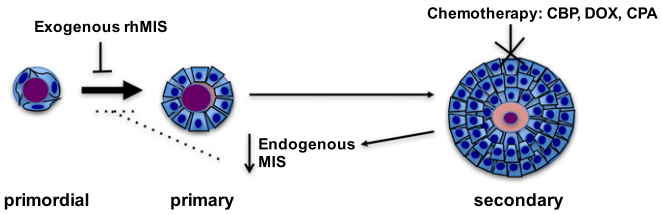


Fig. 6. Model of hormone-replacement treatment with exogenous MIS to protect the ovarian reserve from primordial follicle depletion induced by chemotherapy. Chemotherapeutic agents (CBP, DOX, CPA), which are toxic to the dividing cells of growing follicles, disrupt the negative feedback that such follicles normally provide to inhibit primordial follicle recruitment, leading to a self-amplifying depletion of the ovarian reserve. By restoring negative feedback with exogenous MIS, primordial follicle activation was inhibited, thus lessening the depletion of the ovarian reserve.

mice per group for the experiment shown in Fig. 3*B*, and $n = 5$ mice per group for each experiment of Fig. 5.

Blood Sampling. Mouse blood taken by pricking facial veins or by cardiac puncture at end point, was collected in an Edta 2Na tube, and centrifuged at 900 × *g* for 10 min. Serum was taken from the supernatant and stored at −20 °C until analysis. For frequently repeated, small-volume blood sampling, lateral tail blood was collected; 10 μL was collected and diluted immediately in 90 μL of 1% BSA/PBS, centrifuged, and stored as described above. Blood samples for the murine P4/E2/LH/FSH/InhB ELISAs were taken following the 6-mo mating study, between days 232 and 309. Samples for each test were taken from individual mice ($n = 5$) within 3 d of each other, when their vaginal smears consisted only of cornified epithelium, a cytology normally typical of estrus. Blood samples for the murine MIS ELISA were taken from $n = 3$ mice at the beginning of the study and after chemotherapy (day 14) in mice treated with saline, DOX, CBP, and CPA.

Vaginal Cycling. Female mice were cohoused in groups of four with male bedding, and vaginal smears were taken once a day, at least 5 d/wk, between 10 AM and 11 AM. Dried smears were stained with Giemsa (Sigma Aldrich) for 15 min, rinsed with distilled water, dried at room temperature, and coverslipped with Cytoseal 60 (Thermo Fisher Scientific). The slides were examined by two observers under a light microscope, and the stage of the cycle was determined according to the Allen criteria (65). To compare the time spent in estrus versus other stages, the cycling period was divided in two intervals: from 1 d after the injection (day 1) to day 35 and from day 36 to day 70, and the ratios of days spent in estrus were compared.

ELISA. The ELISA to measure human MIS was performed as previously reported (21). Briefly, a 96-well plate was coated with mouse monoclonal anti-human recombinant MIS antibody (clone 6E11) overnight at 4 °C and was blocked with 1% BSA/PBS and Tween 20 (PBST) (Jackson ImmunoResearch) for 2 h at room temperature. The MIS standard and samples were added to the wells and incubated overnight at 4 °C. The rabbit polyclonal anti-MIS antibody MGH6 was then added and incubated for 1 h at room temperature, and then donkey anti-rabbit IgG antibody conjugated to horseradish peroxidase (HRP) (Jackson ImmunoResearch) was added and incubated for 1 h at 4 °C. The plate was developed using 3,3′,5,5′-Tetramethylbenzidine (TMB) (Sigma Aldrich), and the light absorbance was read at 595 nm in a microplate reader (Vector2 1420; Perkin-Elmer).

Murine P4/E2/LH/FSH/INHB serum levels were measured with ELISA at the Ligand Assay and Analysis Core of the Center for Research in Reproduction at University of Virginia School of Medicine under a cooperative agreement. Mouse E2 was measured with an ELISA kit from Calbiotech, testosterone was measured with an ELISA kit from IBL-America, LH and FSH were measured with the Endocrine Multiplex Assay from EMD Millipore, and InhB was measured with an ELISA kit from Beckman Coulter. Endogenous murine MIS was measured using an ELISA kit (Cusabio Biotech) according to the manufacturer's instructions in samples from $n = 3$ animals before (day 0) and after (day 15) chemotherapy as described in Fig. 5*D*.

Mating Experiments. The C57BL/6N mice were paired 7 d after the AAV9 virus injection. Each pair comprising one female treated with AAV9 empty vector and one female treated with AAV9-MIS was caged with one experienced breeder male. When a pregnant mouse was identified, it was separated until parturition, the size of the litter was recorded, the pups were removed, and the female was reintroduced to the male. After 5 mo of mating, the female mice were separated for 2 mo and then were mated again to different experienced breeder males for 1 mo at age 12 mo. While the mice were separated, blood samples were taken for endocrine studies.

Chemotherapy Models.

AAV9. Peripubertal 6- to 7-wk-old Nu/Nu mice ($n = 20$) were xenografted s.c. in the right flank with 1 M cells of the ovcar5 ovarian cancer cell line as previously described (22). Once the tumor reached a size of 500 mm^3, 26 d after grafting, mice were injected with AAV9-MIS ($n = 10$) or AAV9-GFP ($n = 10$) at dose of 3e11 particles per mouse. The mice were treated with chemotherapeutics [3 mg/kg of DOX i.v. ($n = 10$) or 80 mg/kg of CBP i.p. ($n = 10$)] or saline 24 h after the AAV injection. A second dose of chemotherapeutic agents was given 7 d after the first dose. The animals were euthanized 3 d (for DOX) or 5 d (for CBP) after the second dose of chemotherapeutics, and the ovaries were recovered and fixed for analysis.

Osmotic pump. Peripubertal 6- to 7-wk-old C57BL/6N mice were surgically implanted in the peritoneal cavity with an osmotic pump (ALZET 1007D; DURECT Corporation) filled with 100 μL of rhMIS (1,200 μg/mL) or saline and then were treated with chemotherapeutics or saline i.p. 1 d after the implantation. A second dose of chemotherapeutic agents was given 7 d after the first dose. The implanted pump was replaced every 7 d except in the doxorubicin experiment, in which the pump was replaced every 5 d. Chemotherapeutic regimens used for this experiment are as follows: DOX: 7.5 mg/kg i.p. followed by 6.0 mg/kg i.p. for the second round; CBP: 60 mg/kg i.p. for both rounds: CPA 60 mg/kg for both rounds. The animals were euthanized 7 d after the second dose of chemotherapeutic agent, and the ovaries were dissected for analysis.

Statistical Analysis. All analyses were performed using Prism 7 (GraphPad). When two groups of data with a known direction were compared, an unpaired one-tailed Student's *t* test was used. When the distribution of data was not normal, a Mann–Whitney test was used for analysis. For four groups of chemotherapy analysis, follicle counts in each were compared by two-way ANOVA for multiple comparisons followed by a Holm–Sidak post hoc test. The breeding experiment was assessed by one-way ANOVA for multiple comparisons followed by a Holm–Sidak post hoc test.

Production of rhMIS Protein. RhMIS protein was purified as previously described (21). Briefly, a CHO-K1 clone stably transfected with the LR-MIS vector was grown in HYPERflasks (Corning), and serum-free conditioned medium collected after 72 h of incubation was concentrated 10–20× using a tangential flow over a size-exclusion membrane. The concentrated medium was incubated with Sepharose beads previously conjugated with an anti-human MIS monoclonal antibody (clone 6E11). Bound rhMIS was serially eluted with a glycine-buffered solution (pH 2.9). The eluates containing high levels of rhMIS protein were dialyzed for 4 h against a 10× volume of PBS. All purified protein was tested for activity in the rat urogenital ridge bioassay and was stored at −80 °C until use.

Production of AAV9 Virus. Recombinant AAV9 (rAAV) viral particles were produced, purified, and titrated as previously described (22). Briefly, HEK293 cells were transfected with an AAV plasmid (pAAV) containing the LR-MIS construct flanked with inverted terminal repeats, and the virus was rescued with plasmids expressing AAV9 capsid proteins and adenoviral helper proteins. Particles of rAAV were sedimented by cesium chloride gradient and purified by dialysis. The rAAV vector titer was quantified by silver staining of capsid proteins and quantitative PCR of the genome copy.

Fetal Rat Urogenital Ridge Bioassay. The rat urogenital organ culture bioassay for MIS was performed as previously described (21, 40). In brief, female embryonic urogenital ridges containing ovary, Wolffian, and Müllerian ducts with intervening mesonephros from timed (E14.5) pregnant Sprague–Dawley rats (Envigo) were dissected and incubated on 2% (wt/vol) agarose gel over CMRL 1066 medium (Thermo Fisher Scientific) supplemented with 10% (vol/vol) female fetal bovine serum, 1% penicillin/streptomycin, 1% L-glutamine, 1% Fungizone (Thermo Fisher Scientific), and 5 nM testosterone (Sigma-Aldrich). After incubation for 72 h in presence of the sample, the specimens were fixed, embedded in paraffin, sectioned, and stained with H&E. The sections then were scored under a light microscope by experienced blinded observers. Cultures were carried out with the purified rhMIS at 5 μg/mL, rhMIS solution recovered from the pumps implanted for 7 d in mice at 5 μg/mL, and commercially available C terminal rhMIS (R&D Systems) at a final concentration of 5 μg/mL.

Surgical Procedures.

Ovarian transplants. Ovarian transplants were performed as previously described (66). Briefly, both the recipient and donor mice were anesthetized, and small incisions were made on the back wall at the level of the kidney. The ovary, oviduct, and the distal part of the uterus were exteriorized, taking care to avoid damage; a small incision was made in the ovarian bursa just large enough to pull the ovary through. The ovary of the donor was carefully resected and introduced into the emptied bursa of the recipient. The ovary and reproductive tract were replaced in the peritoneal cavity, the wound was closed with metal clips, and the mice received postoperative care as described above. Transplantations were performed in this manner from AAV9-MIS–treated mice (60 d after injection) into either AAV9-GFP or AAV9-MIS recipients. The animals were euthanized, and ovaries were examined 12 d after surgery.

Pump implantation. Osmotic pumps were primed before implantation by filling them with either 100 μL of rhMIS (1,200 μg/mL) or saline and were incubated in saline at 37 °C for 3 h. The mice were anesthetized with isoflurane, and the procedure was performed on a heated pad. To implant the pump, a small incision was made on the flank, the osmotic pump was installed in the peritoneal cavity, and the wound was closed with metal clips. Mice were given daily dosing of carprofen analgesic (2.5 mg/mL) by oral gavage (100 μL) before the surgery and daily for 2 d postoperatively.

ACKNOWLEDGMENTS. We thank Rana Suliman, Rahgav Mohan, and Miho Suzuki for their help in performing histological stains and Alessandro Alessandrini for his critical input into the manuscript. This study was funded in part by Grant MG14-S06R from the Michelson Found Animal Foundation (to D.P., P.K.D., and G.G.); a Sudna Gar Fellowship (D.P.); an Innovation Development Award from Massachusetts General Hospital (to D.P. and P.K.D.); the Massachusetts General Hospital Executive Committee on Research (ECOR) (D.P. and P.K.D.); a Massachusetts General Hospital Department of Surgery Award (to P.D.K.); funding from the Austen Fund, the McBride family, and Commons Development (P.K.D.); and royalties from the use of the MIS ELISA in infertility clinics around the world.

1. Baker ML, Metcalfe SA, Hutson JM (1990) Serum levels of Müllerian inhibiting substance in boys from birth to 18 years, as determined by enzyme immunoassay. *J Clin Endocrinol Metab* 70(1):11–15.
2. Hudson PL, et al. (1990) An immunoassay to detect human müllerian inhibiting substance in males and females during normal development. *J Clin Endocrinol Metab* 70(1):16–22.
3. Josso N, Legeai L, Forest MG, Chaussain J-L, Brauner R (1990) An enzyme linked immunoassay for anti-müllerian hormone: A new tool for the evaluation of testicular function in infants and children. *J Clin Endocrinol Metab* 70(1):23–27.
4. Seifer DB, et al. (1993) Gonadotropin-releasing hormone agonist-induced differences in granulosa cell cycle kinetics are associated with alterations in follicular fluid müllerian-inhibiting substance and androgen content. *J Clin Endocrinol Metab* 76(3):711–714.
5. Josso N, Picard JY, Rey R, di Clemente N (2006) Testicular anti-Müllerian hormone: History, genetics, regulation and clinical applications. *Pediatr Endocrinol Rev* 3(4):347–358.
6. Dewailly D, et al. (2014) The physiology and clinical utility of anti-Mullerian hormone in women. *Hum Reprod Update* 20(3):370–385.
7. Jost A (1947) Sur les dérivés mülleriens d'embryons de lapin des deux sexes castrés a 21 jours. *C R Seances Soc Biol Fil* 141(3-4):135.
8. Behringer RR, Finegold MJ, Cate RL (1994) Müllerian-inhibiting substance function during mammalian sexual development. *Cell* 79(3):415–425.
9. Nilsson EE, Schindler R, Savenkova MI, Skinner MK (2011) Inhibitory actions of Anti-Müllerian Hormone (AMH) on ovarian primordial follicle assembly. *PLoS One* 6(5):e20087.
10. Hirobe S, He WW, Lee MM, Donahoe PK (1992) Mullerian inhibiting substance messenger ribonucleic acid expression in granulosa and Sertoli cells coincides with their mitotic activity. *Endocrinology* 131(2):854–862.
11. Teixeira J, et al. (1996) Developmental expression of a candidate Müllerian inhibiting substance type II receptor. *Endocrinology* 137(1):160–165.
12. Baarends WM, et al. (1994) A novel member of the transmembrane serine/threonine kinase receptor family is specifically expressed in the gonads and in mesenchymal cells adjacent to the Müllerian duct. *Development* 120(1):189–197.
13. Baarends WM, et al. (1995) Anti-Müllerian hormone and anti-Müllerian hormone type II receptor messenger ribonucleic acid expression in rat ovaries during postnatal development, the estrous cycle, and gonadotropin-induced follicle growth. *Endocrinology* 136(11):4951–4962.
14. di Clemente N, et al. (1994) Cloning, expression, and alternative splicing of the receptor for anti-Müllerian hormone. *Mol Endocrinol* 8(8):1006–1020.
15. Connolly DC, et al. (2003) Female mice chimeric for expression of the simian virus 40 TAg under control of the MISIIR promoter develop epithelial ovarian cancer. *Cancer Res* 63(6):1389–1397.
16. Durlinger AL, et al. (1999) Control of primordial follicle recruitment by anti-Müllerian hormone in the mouse ovary. *Endocrinology* 140(12):5789–5796.
17. Gigli I, Cushman RA, Wahl CM, Fortune JE (2005) Evidence for a role for anti-Mullerian hormone in the suppression of follicle activation in mouse ovaries and bovine ovarian cortex grafted beneath the chick chorioallantoic membrane. *Mol Reprod Dev* 71(4):480–488.
18. Nilsson E, Rogers N, Skinner MK (2007) Actions of anti-Mullerian hormone on the ovarian transcriptome to inhibit primordial to primary follicle transition. *Reproduction* 134(2):209–221.
19. Ragin RC, Donahoe PK, Kenneally MK, Ahmad MF, MacLaughlin DT (1992) Human Müllerian inhibiting substance: Enhanced purification imparts biochemical stability and restores antiproliferative effects. *Protein Expr Purif* 3(3):236–245.
20. Lorenzo HK, et al. (2002) New approaches for high-yield purification of Müllerian inhibiting substance improve its bioactivity. *J Chromatogr B Analyt Technol Biomed Life Sci* 766(1):89–98.
21. Pépin D, et al. (2013) An albumin leader sequence coupled with a cleavage site modification enhances the yield of recombinant C-terminal Mullerian Inhibiting Substance. *Technology* 1(1):63–71.
22. Pépin D, et al. (2015) AAV9 delivering a modified human Mullerian inhibiting substance as a gene therapy in patient-derived xenografts of ovarian cancer. *Proc Natl Acad Sci USA* 112(32):E4418–E4427.
23. Gupta SK, Malik A, Arukha AP (2015) Ovarian and oocyte targets for development of female contraceptives. *Expert Opin Ther Targets* 19(11):1433–1446.
24. Pelosi E, Forabosco A, Schlessinger D (2015) Genetics of the ovarian reserve. *Front Genet* 6:308.
25. Knight PG, Glister C (2006) TGF-β superfamily members and ovarian follicle development. *Reproduction* 132(2):191–206.
26. Morgan S, Anderson RA, Gourley C, Wallace WH, Spears N (2012) How do chemotherapeutic agents damage the ovary? *Hum Reprod Update* 18(5):525–535.
27. Hudson MM (2010) Reproductive outcomes for survivors of childhood cancer. *Obstet Gynecol* 116(5):1171–1183.
28. Green DM, et al. (2009) Ovarian failure and reproductive outcomes after childhood cancer treatment: Results from the Childhood Cancer Survivor Study. *J Clin Oncol* 27(14):2374–2381.
29. El Hachem H, Atallah D, Grynberg M (2014) Fertility preservation in breast cancer patients. *Future Oncol* 10(10):1767–1777.
30. Woodruff TK (2007) The emergence of a new interdiscipline: Oncofertility. *Cancer Treat Res* 138:3–11.
31. Jeruss JS, Woodruff TK (2009) Preservation of fertility in patients with cancer. *N Engl J Med* 360(9):902–911.
32. Lobo RA (2005) Potential options for preservation of fertility in women. *N Engl J Med* 353(1):64–73.
33. Moore HCF, et al.; POEMS/S0230 Investigators (2015) Goserelin for ovarian protection during breast-cancer adjuvant chemotherapy. *N Engl J Med* 372(10):923–932.
34. Elgindy E, Sibai H, Abdelghani A, Mostafa M (2015) protecting ovaries during chemotherapy through gonad suppression: A systematic review and meta-analysis. *Obstet Gynecol* 126(1):187–195.
35. Lambertini M, et al. (2015) Ovarian suppression using luteinizing hormone-releasing hormone agonists during chemotherapy to preserve ovarian function and fertility of breast cancer patients: A meta-analysis of randomized studies. *Ann Oncol* 26(12):2408–2419.
36. Oktay K, Briggs D, Gosden RG (1997) Ontogeny of follicle-stimulating hormone receptor gene expression in isolated human ovarian follicles. *J Clin Endocrinol Metab* 82(11):3748–3751.
37. Lee MM, et al. (1997) Measurements of serum müllerian inhibiting substance in the evaluation of children with nonpalpable gonads. *N Engl J Med* 336(21):1480–1486.
38. Gustafson ML, et al. (1992) Müllerian inhibiting substance as a marker for ovarian sex-cord tumor. *N Engl J Med* 326(7):466–471.
39. Cate RL, et al. (1986) Isolation of the bovine and human genes for Müllerian inhibiting substance and expression of the human gene in animal cells. *Cell* 45(5):685–698.
40. Price JM, Donahoe PK, Ito Y (1979) Involution of the female Mullerian duct of the fetal rat in the organ-culture assay for the detection of Mullerian Inhibiting Substance. *Am J Anat* 156(2):265–284.
41. Grive KJ, et al. (2016) TAF4b regulates oocyte-specific genes essential for meiosis. *PLoS Genet* 12(6):e1006128.
42. Nelson JF, Felicio LS, Osterburg HH, Finch CE (1981) Altered profiles of estradiol and progesterone associated with prolonged estrous cycles and persistent vaginal cornification in aging C57BL/6J mice. *Biol Reprod* 24(4):784–794.
43. Franks LM, Payne J (1970) The influence of age on reproductive capacity in C57BL mice. *J Reprod Fertil* 21(3):563–565.
44. Jamin SP, Arango NA, Mishina Y, Hanks MC, Behringer RR (2002) Requirement of Bmpr1a for Müllerian duct regression during male sexual development. *Nat Genet* 32(3):408–410.
45. Xu J, Bishop CV, Lawson MS, Park BS, Xu F (2016) Anti-Müllerian hormone promotes pre-antral follicle growth, but inhibits antral follicle maturation and dominant follicle selection in primates. *Hum Reprod* 31(7):1522–1530.
46. Schmidt KLT, Kryger-Baggesen N, Byskov AG, Andersen CY (2005) Anti-Müllerian hormone initiates growth of human primordial follicles in vitro. *Mol Cell Endocrinol* 234(1-2):87–93.
47. Durlinger ALL, et al. (2002) Anti-Müllerian hormone inhibits initiation of primordial follicle growth in the mouse ovary. *Endocrinology* 143(3):1076–1084.
48. Cimino I, et al. (2016) Novel role for anti-Müllerian hormone in the regulation of GnRH neuron excitability and hormone secretion. *Nat Commun* 7:10055.
49. Garrel G, et al. (2016) Anti-Müllerian hormone: A new actor of sexual dimorphism in pituitary gonadotrope activity before puberty. *Sci Rep* 6:23790.
50. Takahashi M, Koide SS, Donahoe PK (1986) Müllerian inhibiting substance as oocyte meiosis inhibitor. *Mol Cell Endocrinol* 47(3):225–234.
51. Andersen CY, et al. (2010) Concentrations of AMH and inhibin-B in relation to follicular diameter in normal human small antral follicles. *Hum Reprod* 25(5):1282–1287.
52. Li J, et al. (2015) Vectored antibody gene delivery mediates long-term contraception. *Curr Biol* 25(19):R820–R822.
53. Hamy A-S, et al. (2014) Ovarian reserve in breast cancer: Assessment with anti-Müllerian hormone. *Reprod Biomed Online* 29(5):573–580.
54. Li X, Kang X, Deng Q, Cai J, Wang Z (2013) Combination of a GnRH agonist with an antagonist prevents flare-up effects and protects primordial ovarian follicles in the rat ovary from cisplatin-induced toxicity: A controlled experimental animal study. *Reprod Biol Endocrinol* 11:16.
55. Morgan S, Lopes F, Gourley C, Anderson RA, Spears N (2013) Cisplatin and doxorubicin induce distinct mechanisms of ovarian follicle loss; imatinib provides selective protection only against cisplatin. *PLoS One* 8(7):e70117.
56. Kalich-Philosoph L, et al. (2013) Cyclophosphamide triggers follicle activation and "burnout"; AS101 prevents follicle loss and preserves fertility. *Sci Transl Med* 5(185):185ra62.
57. van der Kaaij MAE, van Echten-Arends J, Simons AHM, Kluin-Nelemans HC (2010) Fertility preservation after chemotherapy for Hodgkin lymphoma. *Hematol Oncol* 28(4):168–179.
58. Yuksel A, et al. (2015) The magnitude of gonadotoxicity of chemotherapy drugs on ovarian follicles and granulosa cells varies depending upon the category of the drugs and the type of granulosa cells. *Hum Reprod* 30(12):2926–2935.
59. McAllister JM, Legro RS, Modi BP, Strauss JF, 3rd (2015) Functional genomics of PCOS: From GWAS to molecular mechanisms. *Trends Endocrinol Metab* 26(3):118–124.
60. Sullivan SD, Welt C, Sherman S (2011) FMR1 and the continuum of primary ovarian insufficiency. *Semin Reprod Med* 29(4):299–307.
61. Gavish Z, Peer G, Roness H, Cohen Y, Meirow D (2014) Follicle activation and 'burnout' contribute to post-transplantation follicle loss in ovarian tissue grafts: The effect of graft thickness. *Hum Reprod* 29(5):989–996.
62. Jensen AK, et al. (2017) Cryopreservation of ovarian tissue for fertility preservation in a large cohort of young girls: Focus on pubertal development. *Hum Reprod* 32(1):154–164.
63. Committee on Care and Use of Laboratory Animals (2011) *Guide for the Care and Use of Laboratory Animals* (National Academies Press, Washington, DC), 8th Ed.
64. Pépin D, Paradis F, Perez-Iratxeta C, Picketts DJ, Vanderhyden BC (2013) The imitation switch ATPase Snf2l is required for superovulation and regulates Fgl2 in differentiating mouse granulosa cells. *Biol Reprod* 88(6):142.
65. Allen E (1922) The oestrous cycle in the mouse. *Am J Anat* 30(3):297–371.
66. Nagy A (2002) *Manipulating the Mouse Embryo: A Laboratory Manual* (Cold Spring Harbor Lab Press, Cold Spring Harbor, NY), 3rd Ed.

Supporting Information

Kano et al. 10.1073/pnas.1620729114

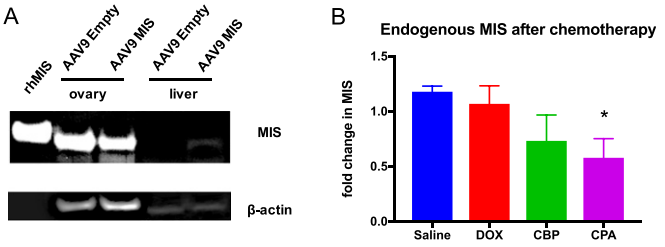


Fig. S1. Expression of MIS in the ovary following AAV9 treatment and chemotherapy-induced changes in endogenous murine MIS. (*A*) Immunoblot of tissue protein lysates from animals treated with AAV9-empty vector or AAV9-MIS probed for the expression of MIS (murine and human) and β-actin. (*B*) Average change in endogenous murine MIS levels, as measured by ELISA, comparing pretreatment and posttreatment serum concentrations (14 d after two weekly doses of saline, DOX, CBP, or CPA) in individual mice ($n = 3$ per group). *$P < 0.05$ by Student's t test compared with saline control.

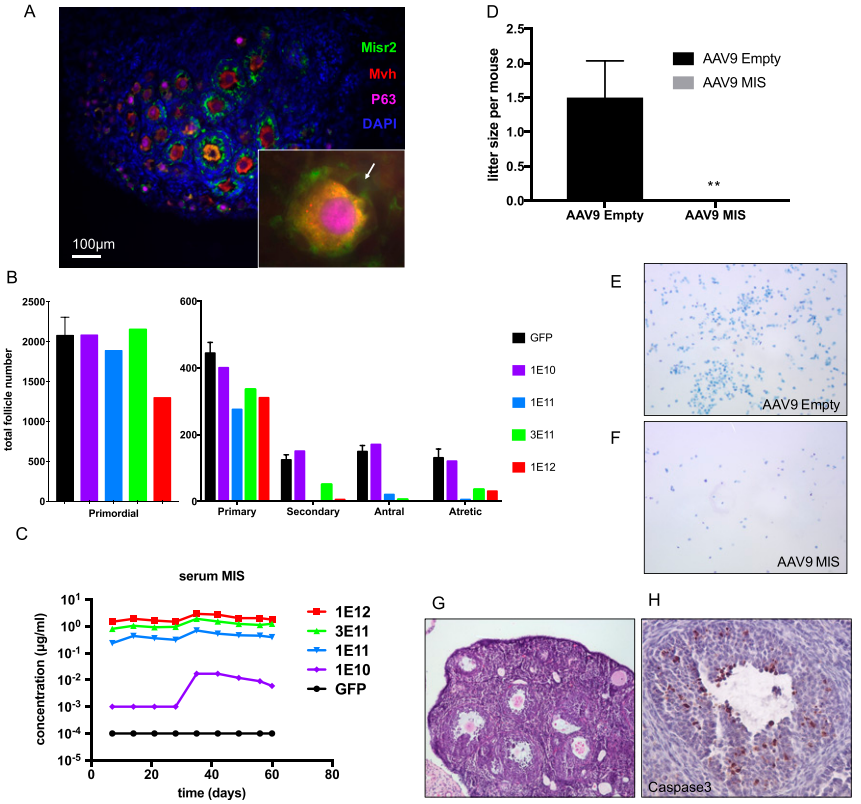


Fig. S2. Validation of the treatment modality. (*A*) Neonatal (postnatal day 7) mouse ovaries were sectioned and stained for Misr2 (green), Mvh (red), P63 (purple), and DAPI (blue). (*Inset*) A representative primordial follicle (DAPI excluded for clarity). (*B*) Total follicle counts 60 d after administration of 1e10–1e12 viral particles of AAV9-MIS or 3e11 particles of GFP (control). (*C*) Viral titrations with serial serum analysis for circulating rhMIS by a human-specific ELISA. (*D*) Average number of pups produced per female during a 1-mo mating period at 12 mo of age in $n = 10$ females treated with either AAV9-MIS or AAV9-empty control at 7 wk of age. **$P < 0.01$ by Student's t test. (*E* and *F*) Representative ($n = 3$) vaginal cytology consisting of cornified epithelium typical of estrus in females treated with (*E*) AAV9-empty vector controls or (*F*) AAV9-MIS at day 70 of treatment. (*G*) A representative middle section from an AAV9-GFP CBP-treated ovary at end point stained by H&E. (Magnification: 40×.) (*H*) Representative cleaved caspase-3 IHC-stained follicle from the same ovary. (Magnification: 100×.)

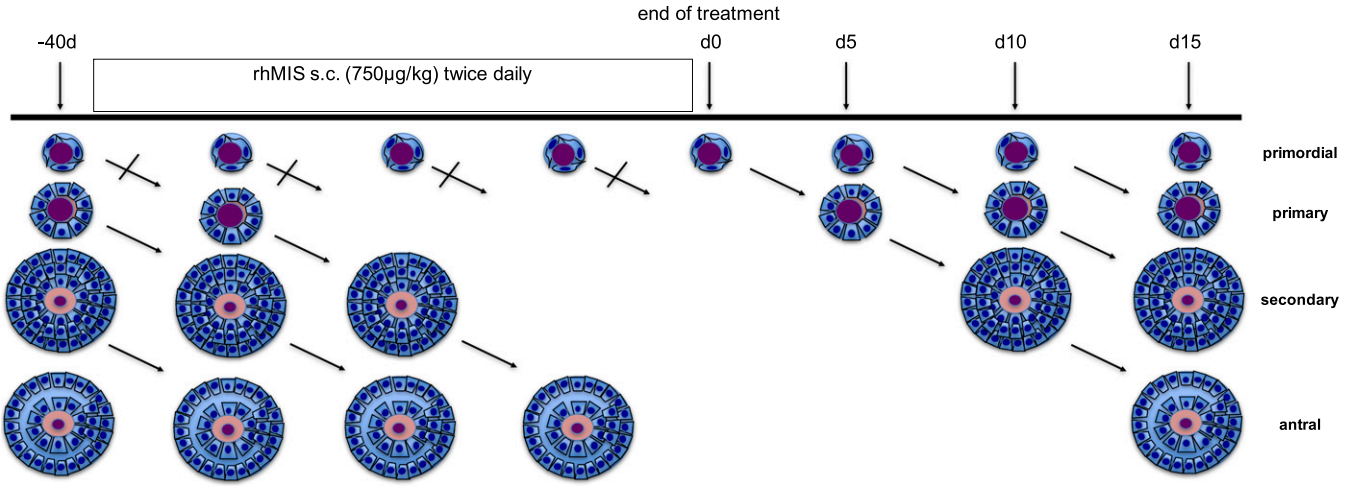


Fig. S3. Model of induced reversible follicle quiescence and reawakening following temporary treatment with MIS protein. Treatment with MIS protein inhibits primordial follicle activation, but already recruited primary, secondary, and antral follicles are committed to continue their irreversible development and are progressively depleted from the ovary. At the conclusion of the treatment period (day 40), the ovary consists entirely of primordial follicles. Cessation of treatment at this step can allow some of the quiescent primordial follicles gradually to resume their progress to the primary, secondary, and antral stages.